AD-A038 048 BALLISTIC RESEARCH LABS ABERDEEN PROVING GROUND MD F/G 20/3
ON THE PHENOMENON OF CURRENT PULSES GENERATED BY CONDUCTORS NEA--ETC(U)
DEC 76 W BUCHER

UNCLASSIFIED BRL-1951 NL

1 OF 1
AD A038048

END

DATE
FILMED
4-77

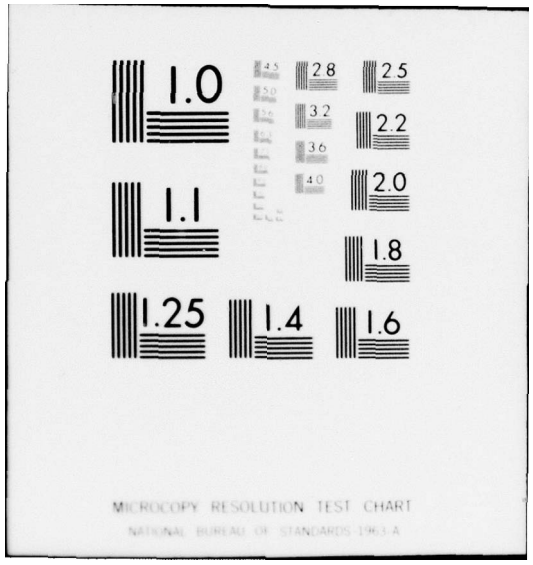
1.0
1.1
1.25
1.4
1.6
1.8
2.0
2.2
2.5
2.8
3.2
3.6
4.0
4.5
5.0
5.6
MICROCOPY RESOLUTION TEST CHART
NATIONAL BUREAU OF STANDARDS 1963-A

BRL R 1951

BRL

AD

REPORT NO. 1951

ON THE PHENOMENON OF CURRENT PULSES GENERATED BY CONDUCTORS NEAR CONTACT IN ELECTRIC FIELDS

William Bucher

December 1976

Approved for public release; distribution unlimited.

USA BALLISTIC RESEARCH LABORATORY
ABERDEEN PROVING GROUND, MARYLAND

Destroy this report when it is no longer needed.
Do not return it to the originator.

Secondary distribution of this report by originating or sponsoring activity is prohibited.

Additional copies of this report may be obtained from the National Technical Information Service, U.S. Department of Commerce, Springfield, Virginia 22151.

The findings in this report are not to be construed as an official Department of the Army position, unless so designated by other authorized documents.

UNCLASSIFIED

SECURITY CLASSIFICATION OF THIS PAGE *(When Data Entered)*

REPORT DOCUMENTATION PAGE

READ INSTRUCTIONS BEFORE COMPLETING FORM

1. REPORT NUMBER: BRL REPORT NO. 1951
2. GOVT ACCESSION NO.
3. RECIPIENT'S CATALOG NUMBER

4. TITLE *(and Subtitle)*: ON THE PHENOMENON OF CURRENT PULSES GENERATED BY CONDUCTORS NEAR CONTACT IN ELECTRIC FIELDS.

5. TYPE OF REPORT & PERIOD COVERED: Final report,

6. PERFORMING ORG. REPORT NUMBER

7. AUTHOR(s): William Bucher

8. CONTRACT OR GRANT NUMBER(s)

9. PERFORMING ORGANIZATION NAME AND ADDRESS
USA Ballistic Research Laboratory
Aberdeen Proving Ground, MD 21005

10. PROGRAM ELEMENT, PROJECT, TASK AREA & WORK UNIT NUMBERS: 1L662618AH80

11. CONTROLLING OFFICE NAME AND ADDRESS
US Army Materiel Development & Readiness Command
5001 Eisenhower Avenue
Alexandria, VA 22333

12. REPORT DATE: December 1976

13. NUMBER OF PAGES: 21

14. MONITORING AGENCY NAME & ADDRESS *(if different from Controlling Office)*: 12 17p.

15. SECURITY CLASS. *(of this report)*: UNCLASSIFIED

15a. DECLASSIFICATION/DOWNGRADING SCHEDULE: N/A

16. DISTRIBUTION STATEMENT *(of this Report)*

Approved for public release; distribution unlimited.

17. DISTRIBUTION STATEMENT *(of the abstract entered in Block 20, if different from Report)*

18. SUPPLEMENTARY NOTES

19. KEY WORDS *(Continue on reverse side if necessary and identify by block number)*

conductors
electric fields
electric pulses
detectors

20. ABSTRACT *(Continue on reverse side if necessary and identify by block number)* (cas)

The generation of current pulses in external circuitry by neutral and charged conductors near contact in electric fields is described. Theoretical predictions are presented for various configurations of fields and conductors. The results are directly applicable to both the detection of conducting particles and conductor linkage.

DD FORM 1 JAN 73 1473 EDITION OF 1 NOV 65 IS OBSOLETE

UNCLASSIFIED 050 750

SECURITY CLASSIFICATION OF THIS PAGE *(When Data Entered)*

TABLE OF CONTENTS

LIST OF FIGURES

1. INTRODUCTION

Given two electrodes with constant potential difference, a conducting body (either neutral or charged) will, upon approaching either electrode, case a sharp rise in the current flowing in the external circuit immediately before contacting the electrode. A simular pulse will also result from two conductors approaching each other in the field produced by the electrodes. These effects are of particular interest in the detection of conducting particles and in the detection of linkage-chain formation across electrode gaps.

2. GENERAL CONSIDERATIONS

A conductor traversing the region between the electrodes will result in an energy exchange among, 1) the kinetic energy of the conductor, 2) the total electrostatic field energy, and 3) the external energy source, e.g., a battery. This energy exchange is associated with the motion of the conductor, and thus current flow in the external circuit occurs only during the traversal and ceases upon contact. The charge distribution on the surface of the conductor changes continuously during traversal, and as the electrode is approached, a charge concentration which approaches a delta function $\delta(x - 0)$ is formed on that part of the conductor nearest to the electrode. Upon contact, this delta function of charge is annihilated by an image charge at the electrode surface. However, this transfer of charge from the conductor to the electrode occurs without energy exchange and hence without current flow in the external circuit.

As an example of the above process of pulse generation, the case of a neutral conductor between two parallel plates is especially illustrative. It can be shown[1] that the attraction of the conductor by its infinite set of image charges results in the external energy flow being equally partitioned between the electrostatic field energy and the kinetic energy. Nearly all of this energy change occurs typically within a few microns of contact and is directly associated with the change in the charge distribution on the conductor which causes a peaking of the displacement current ($\partial D/\partial t$). By Kirchhoff's Law, the current in the external circuit is equal to the displacement current and hence is identically peaked. By means of the Energy Partition Theorem of reference (1), the external current is easily inferred from a knowledge of the net force F on the conductor:

$$2F\,dx = V\,dQ_{ext} \qquad (1)$$

or

$$I_{ext}/u = 2F/V,$$

[1] W. Bucher, "Energy Partition", BRL Report in preparation.

where u is the velocity and V is the potential difference between the plates. The force F on a long, thin conductor has been derived (see reference 2). For this case, the external current flow is given by,

$$I_{ext}(z)/u = - \frac{q_o^2}{\gamma V} \frac{\frac{\partial}{\partial Z} \phi(z)}{[1 + \beta(\phi(Z) + G)]^2} \qquad (2)$$

where $\phi(z)$ is the bipolar potential-energy function, which takes into account the effects of the infinite set of images that are generated through multiple reflections by the parallel plates; G is a geometric potential function independent of z; and q_o is the classical charge separation factor for a conductor in a uniform field, i.e., in the absence of the conducting plates. The square of the factor in brackets in the denominator of eq. 2 takes into account the effects of the plates in enhancing the charge separation. Figure 1 is a plot of the function $I_{ext}(Z)/u$ for a long, thin cylindrical conductor. A plot for an ellipsoidal conductor of comparable dimensions would be nearly identical except within the region of a few microns from contact. The essential difference is that I(Z) is finite as $Z \rightarrow \pm d/2$ for flat-ended conductors and infinite for conductors with rounded ends; however the areas under the curves are necessarily the same.

2.1 Coherent Acceleration

The region within approximately 0.1 microns of contact is characterized by enormous accelerations, which for thin neutral conductors can, in principle, amount to several billion g's for moderate plate supply voltages. The mechanism underlying this acceleration is based on coherence. Coherence is implicit in the nature of image forces, such forces being proportional to the square of the clustered charge. The clustering process is automatic, being achieved in the formation of a one-dimensional delta function at one end of the conductor. In 1956 Veksler proposed[3] the use of the coherence principle as a means of attaining high accelerations in particle accelerators and outlines four basic ways in which coherence forces could result on particle clusters. From the above it is apparent that image forces represent another way of coherent acceleration.

2.2 Charge Pulses

In the region of coherent acceleration, sparking may occur across the submicron conductor-electrode gap. In this case the remaining gain in kinetic energy is not realized but instead is dissipated in the form

---

[2] W. Bucher, "Motion of Conductors in Electrostatic Field", BRL Report in preparation.

[3] V.I. Veksler, "Proceedings of the CERN Symposium on High Energy Accelerators", GENEVA, 1956 (CERN Scientific Information Service, Geneva, 1956), Vol. 1, p. 80.

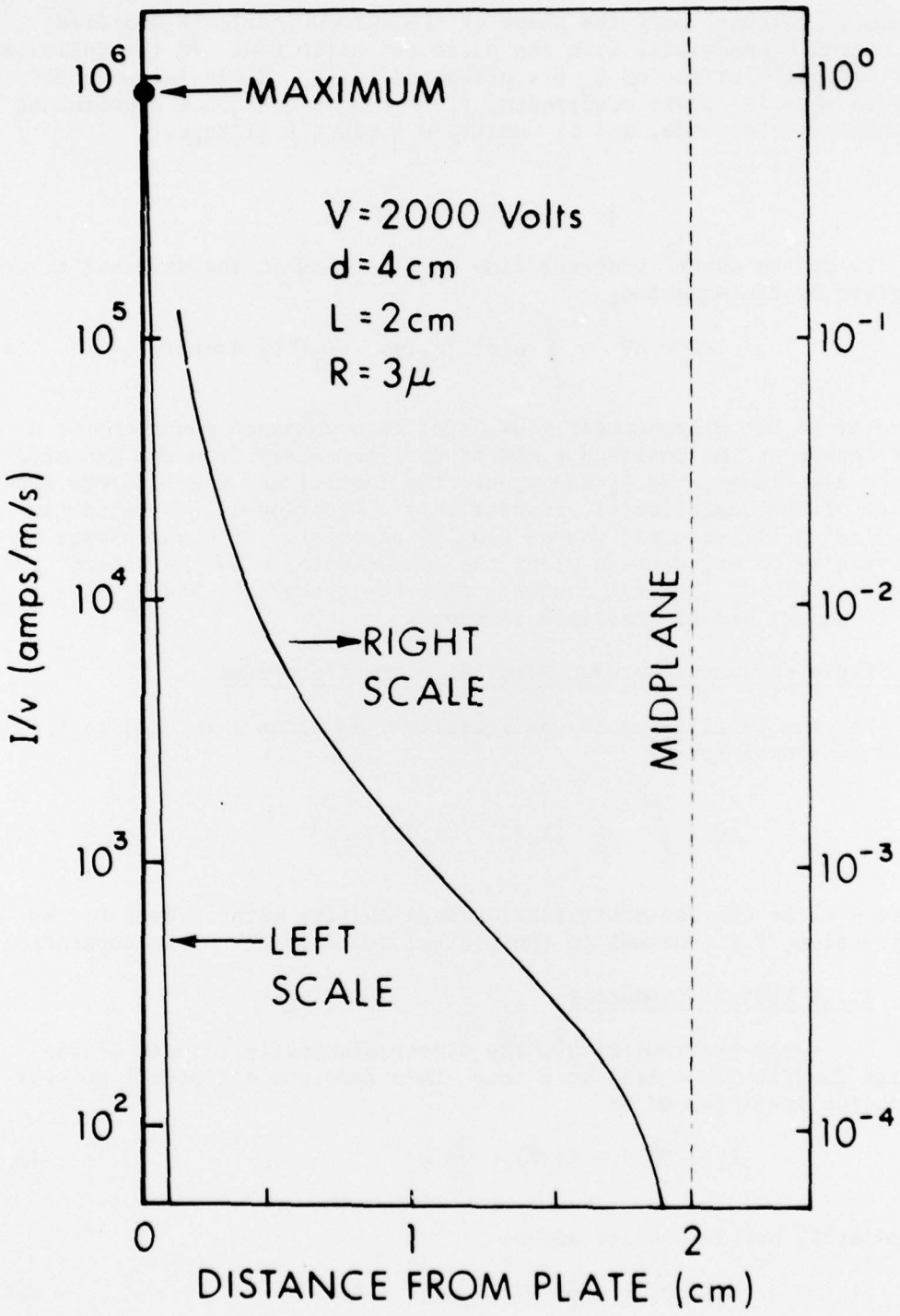

Figure 1. Displacement Current Per Unit Velocity Versus Position of an Uncharged, Cylindrical (namely, Flat-Ended) Conductor Moving in the Electric Field Between Parallel Plate Electrodes.

of heat. However, only the shape of the current pulse is modified; the charge Q_p associated with the pulse is uneffected. In the following section, calculations of Q_p are presented for 1) a single conductor between parallel plate electrodes, 2) a single conductor approaching a spherical electrode, and 3) multiple conductor linkage.

3. CALCULATIONS OF Q_p

It can be shown[1] that the flow of charge ΔQ in the external circuit is given by the equation,

$$\Delta Q = \Delta \Psi = \int w(r) \, [\rho_f(r) - \rho_i(r)] \, dxdydz, \tag{3}$$

where $\Delta \Psi$ is the displacement flux, $w(r)$ is a response function for a unit charge at the position r and is derived solely from the geometry of the electrodes, and ρ_i and ρ_f are the initial and final charge densities of the conductor(s), respectively. Equation (3) is valid for calculating the external charge flow ΔQ associated with any change in position(s) or orientation(s) of the conductor(s). In the present work however, only Q_t (the total charge flow per traversal) and Q_p (the charge pulse) are of immediate interest.

3.1 Single Conductor Between Parallel Plate Electrodes

For the parallel plate configuration, equation 1 reduces to the one-dimensional form

$$\Delta Q = \int_0^d \frac{z}{d} \, [\lambda_f(Z) - \lambda_i(Z)] \, dz \tag{4}$$

where $\lambda(Z)$ is the one-dimensional charge density with respect to the Z direction, i.e., normal to the plates, and d is the plate separation.

3.1.1 Neutral Conductor

From previous work[2], the electrostatically induced linear charge distributions $\lambda(Z)$ on a long, thin (prolate ellipsoid) neutral conductor are inferred as

$$\lambda_f(Z,0) = - q\delta(Z) + \frac{2q}{L^2} Z \tag{5}$$

immediately before contact and as

$$\lambda_i(Z,b) = - \frac{4q}{L} + \frac{8q}{L^2} (Z - b) \tag{6}$$

for $b \geq 100\ R$, where b is the distance between the conductor and electrode and R is the radius of the conductor. In the above equations, L is the conductor length, and q is the net charge the conductor would acquire upon contact and is given by*

$$q = \pi\varepsilon_o E_o L^2/[\ell n \left(\frac{2L}{R}\right) - 1], \tag{7}$$

where $E_o = V/d$ and V is the constant potential difference between the electrodes. The distributions $\lambda(Z)$ are shown in Figure 2a. The essential point in the above is that the surface charge distribution on the conductor does not change significantly except in the immediate proximity of the electrode, namely, for $b \leq 100\ R$, the region of pulse formation.

The result of the above indicated integration for Q_p corresponding to a neutral conductor approaching either plate is

$$\begin{aligned} Q_p = \Delta Q &= Lq/2d \\ &= \pi\varepsilon_o E_o L^3/2d[\ell n \left(\frac{2L}{R}\right) - 1]. \end{aligned} \tag{8}$$

3.1.2 Charged Conductor

The appropriate linear charge distributions for a long, thin conductor carrying a net charge -q, acquired from contacting the opposite plate (given by Eq. 7), are shown in Figure 2b. The results for Q_p, the charge pulse, and Q_t, the total charge flow per traversal, are

$$Q_T = q \tag{9}$$

$$\begin{aligned} Q_p &= Lq/d \\ &= \pi\ \varepsilon_o E_o L^3/d\ [\ell n \left(\frac{2L}{R}\right) - 1] \end{aligned} \tag{10}$$

3.2 Single Conductor Approaching a Spherical Electrode

For the case of a single spherical electrode, Eq. 3 can be reduced to the one-dimensional radial form

$$\Delta Q = \int_a^\infty w(r)\ [\lambda_f(r) - \lambda_i(r)]\ dr. \tag{11}$$

*Note: When the conductor length is comparable to the plate separation, the charge enhancement correction of reference 1 must be used. Otherwise, the enhancement factor is 1.00 as shown in equation 7 and subsequent equations.

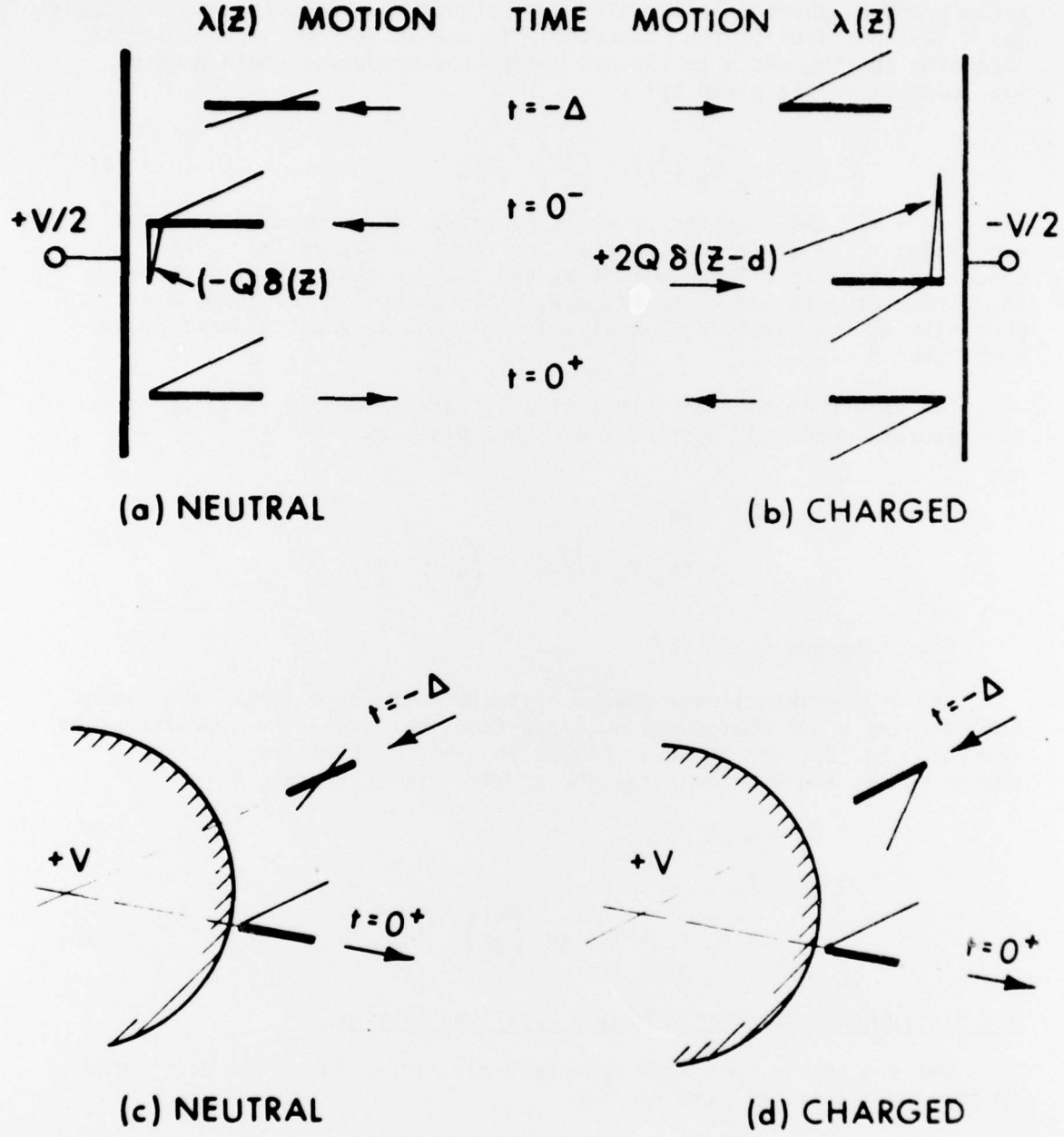

Figure 2. Linear Charge Distributions on Long, Thin Conductors in Region of Electrodes.

The normalized weighting function w(r) is determined from elementary considerations of displacement flux to be

$$w(r) = -a/(a + r) + \text{const.}, \tag{12}$$

where a is the radius of the electrode.

3.2.1 Neutral Conductor

The appropriate linear charge distributions for a long, thin neutral conductor approaching the spherical conductor of constant absolute potential V_o are shown in Figure 2c. Here, q_o represents the net charge the conductor would acquire upon contact and is given to good accuracy by

$$q_o = \pi\varepsilon_o V_o \, aL^2/[a + \tfrac{2}{3}L]^2 \, [\ell n \, (\tfrac{2L}{R}) - 1] \quad \text{for } L < a. \tag{13}$$

The result for Q_p is

$$Q_p = q_o \left[1 - \frac{\ell n(1 - \alpha)}{\alpha}\right]$$

$$= \frac{3\pi\varepsilon_o V_o L^2 \left[1 - \dfrac{\ell n\,(1 - \alpha)}{\alpha}\right]}{2a(\tfrac{3}{2} + \alpha)^2 \, [\ell n \, (\tfrac{2L}{R}) - 1]}, \tag{14}$$

where

$$\alpha = L/a.$$

3.2.2 Charged Conductor

Figure 2d shows the charge distributions for a long thin conductor carrying a net charge $-q_o$ (acquired, for example, from contacting a similar spherical electrode at a remote location and at an absolute potential $-V_o$). The result for the external charge pulse is

$$Q_p = 2q_o \left[1 - \frac{(\ell n \, (1 + \alpha)}{\alpha}\right], \tag{15}$$

which is twice that for the case of the neutral conductor given in Eq. (14).

3.3 Linkage of Conductors Between Parallel Plate Electrodes

Figure 3a shows the equilibrium positions for N identical neutral conductors across the electrode gap. However, this equilibrium is unstable, and a small displacement of any conductor will cause an imbalance of the image forces and lead to collisions. A collision between two neutral conductors (N-N) will result in a charge pulse through the external circuit

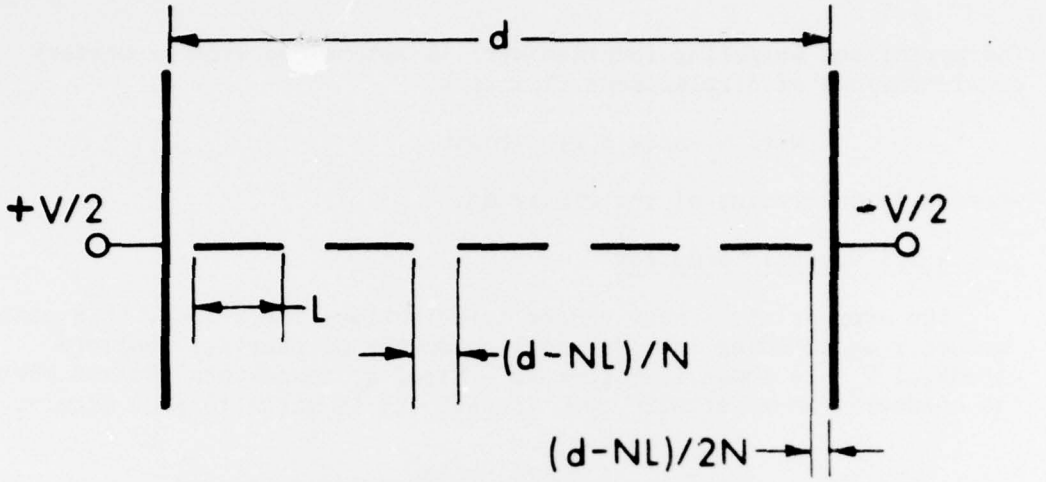

(a) EQUILIBRIUM POSITION FOR N CONDUCTORS

(b) TYPE N-N COLLISION

(c) TYPE C-N COLLISION

(d) TYPE C-C COLLISION

Figure 3. Conductor Linkage Across Electrode Gap.

Q_p nn and subsequently an exchange of charge between conductors. Basically, this pheonmenon is the same as that of a single conductor striking the electrode and therefore Equations 3 and 4 are applicable.

Following the N-N collisions (see Figure 3b), two other types of interactions will occur: N-C and C-C collisions, as shown in Figures 3c and d, respectivley. After a number of collisions, only the type C-C are possible. For each of these three interactions, the charge pulse Q_p is calculated as follows.

3.3.1 N-N Collisions

From Equation 4 and the [redacted] charge distributions of Figure 3b, the charge pulse is determined to be

$$Q_p^{NN} = Lq/d \tag{16}$$

where q is defined as in Equation 7.

3.3.2 N-C Collisions

From Equation 4 and the [redacted] charge distibutions of Figure 3c the charge pulse is determined to be

$$Q_p^{NC} = 3Lq/2d. \tag{17}$$

3.3.3 C-C Collisions

From Equation 4 and the [redacted] charge distributions of Figure 3d the charge pulse is determined to be

$$Q_p^{CC} = 2Lq/d. \tag{18}$$

4. SUMMARY

It is clear from Sections 2 and 3 that the process of generating current pulses in external circuitry is now well understood.

The quantitative results for long, thin conductors are summarized in Figure 4 and 5 for the parallel plate and the spherical electrode configurations, respectively. Table 1 lists the results for conductor linkage across electrode gaps.

Only for the parallel plate geometry are experimental data available for comparison. Morrissey and Brannon[4] have measured the charge pulses

[4] J. Morrissey and W. Brannon, BRL Report to be published.

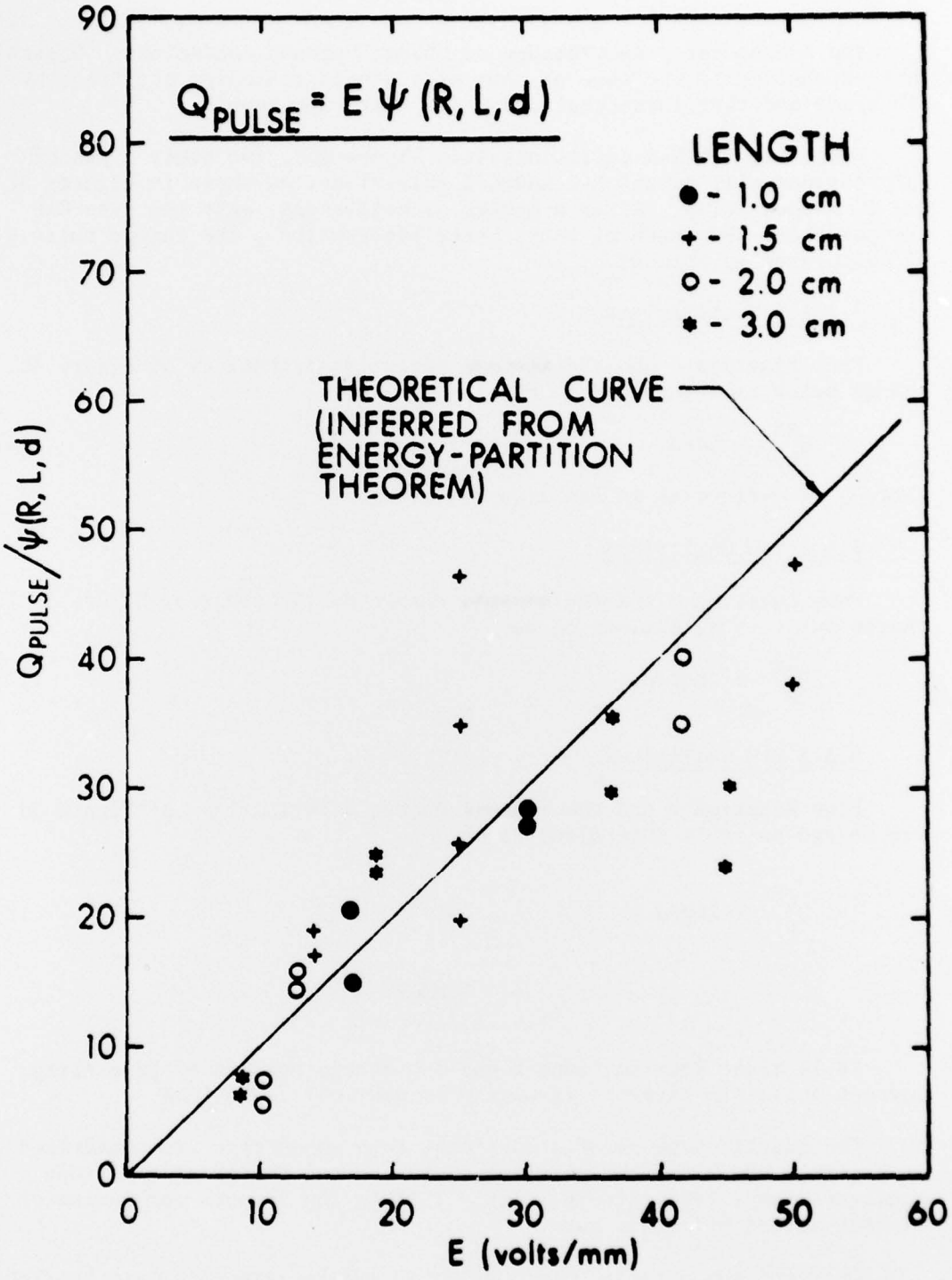

Figure 4. Q_p Pulses Generated by a Long, Thin Conductor Approaching a Parallel Plate Electrode. The Data Points Were Taken for a Variety of Conductor Lengths L and Gap Widths d (see test for Functional Dependence $\Psi(R,L,d)$).

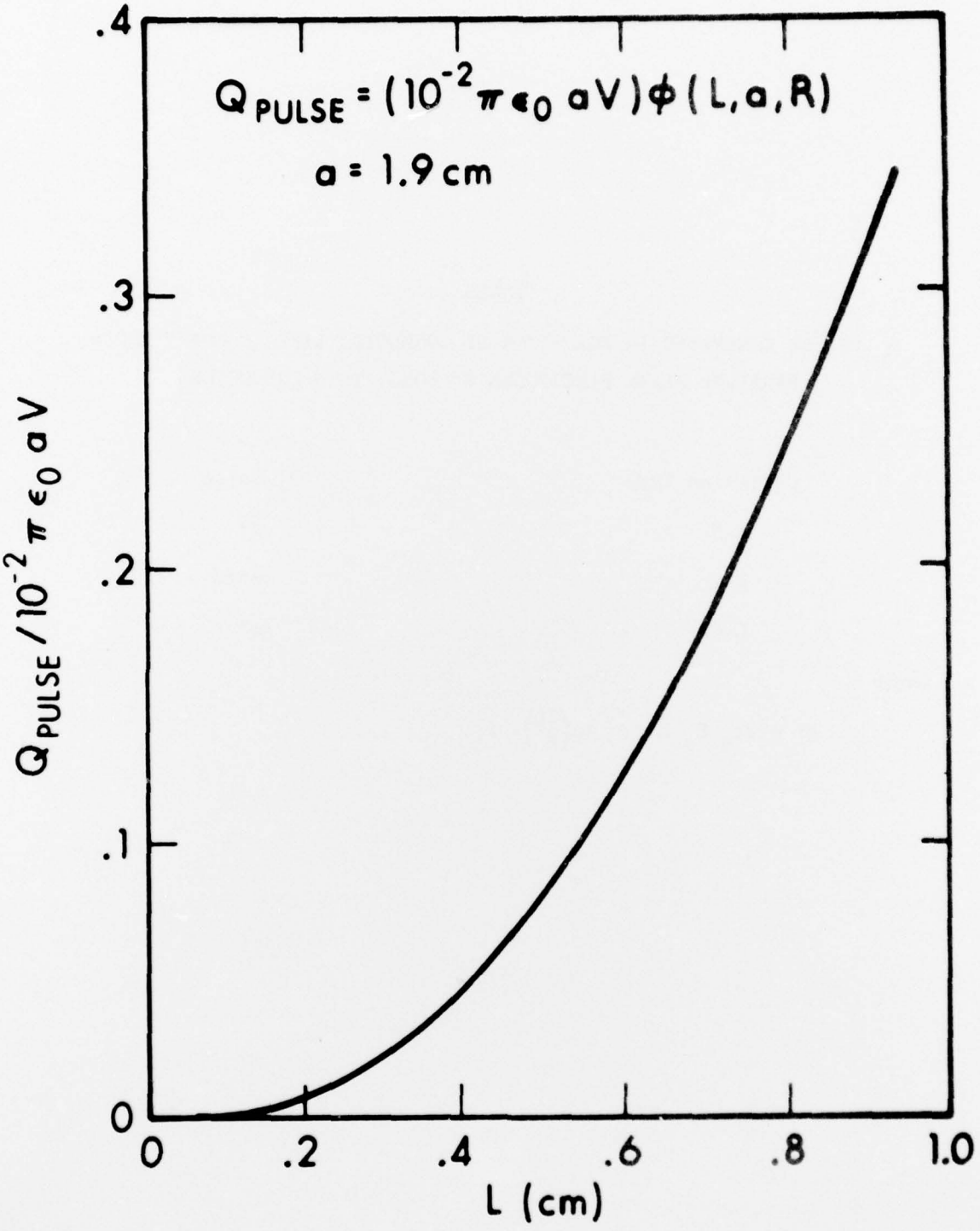

Figure 5. Q_p Pulses Generated by a Long, Thin Conductor Approaching a Spherical Electrode. See test for Functional Dependence $\phi(L,a,r)$.

TABLE 1

Q_p PULSES GENERATED IN FORMATION OF CONDUCTOR LINKAGE CHAIN ACROSS PARALLEL PLATE ELECTRODES BY LONG, THIN CONDUCTORS

Collision Type	Q_p Pulse
N-N	q^*
N-C	$3q^*/2$
C-C	$2q^*$

where

$$q^* = \pi\varepsilon_o E_o L^3/d\left[\ln\left(\frac{2L}{R}\right) - 1\right].$$

Q_p for a variety of electrode separations d, electric field strengths E_o, and conductor lengths L. All these data points, which are folded into the one-dimensional plot of Figure 4, are in agreement with the calculated curve. (To avoid possible confusion, please note that in the graphical method used in reference 4 for displaying the data, the data points do not and should not lie on a single curve since various values of d and L are represented. In Figure 4 of the present report, however, the single curve representation is applicable).

The calculated curve of Figure 5 for the spherical electrode configuration is of particular practical importance in the detection of conducting particles.[5] From this curve can be inferred the conductor length as a function of the detected pulse-height. Preliminary measurements with the spherical detector[6] show excellent agreement with the above curve.

Concerning coherent acceleration in the near region of the electrodes, it is noted that sparking limited the kinetic energy acquired by the conductor during the pulse to approximately 30 percent of its optimum value. This was inferred from the observed shape of the external current pulse.

ACKNOWLEDGEMENTS

I thank Mr. John Morrissey and Mr. William Brannon for discussions concerning their many and varied measurements, and Dr. Russell D. Shelton for discussions and encouragement in this effort.

[5] R. Shelton and J. Morrissey, "Airborne Particle Analyzer", Patent Pending.

[6] Private Communication with J. Morrissey and W. Brannon.

DISTRIBUTION LIST

No. of Copies	Organization
12	Commander Defense Documentation Center ATTN: DDC-TCA Cameron Station Alexandria, VA 22314
1	Commander US Army Materiel Development and Readiness Command ATTN: DRCDMA-ST 5001 Eisenhower Avenue Alexandria, VA 22333
1	Commander US Army Aviation Systems Command ATTN: DRSAV-E 12th and Spruce Streets St. Louis, MO 63166
1	Commander US Army Air Mobility Research and Development Laboratory Ames Research Center Moffett Field, CA 94035
1	Commander US Army Electronics Command ATTN: DRSEL-RD Fort Monmouth, NJ 07703
1	Commander US Army Missile Research and Development Command ATTN: DRDMI-R Redstone Arsenal, AL 35809
1	Commander US Army Tank Automotive Development Command ATTN: DRDTA-RWL Warren, MI 48090
2	Commander US Army Mobility Equipment Research & Development Command ATTN: Tech Docu Cen, Bldg. 315 DRSME-RZT Fort Belvoir, VA 22060
1	Commander US Army Armament Materiel Readiness Command Rock Island, IL 61202
1	Commander US Army Harry Diamond Labs ATTN: DRXDO-TI 2800 Powder Mill Road Adelphi, MD 20783
1	Director US Army TRADOC Systems Analysis Activity ATTN: ATAA-SA White Sands Missile Range NM 88002
	Aberdeen Proving Ground
	Marine Corps Ln Ofc Dir, USAMSAA